ARTICLE

Improving the steric hindrance effect of linear sulfonated acetone-formaldehyde dispersant and its performance in coal-water slurry

Received 00th January 20xx,
Accepted 00th January 20xx

DOI: 10.1039/x0xx00000x

Wenlin Shuai,[abc] Shiwei Wang,*[b] Taotao Sun,[b] Hongfeng Yin,[b] Yu Zu,[b] Gang Yao,[d] Zhonghua Li,[d] Zhaokun Qi [d] and Mei Zhong *[ac]

[a.] *State Key Laboratory of Chemistry and Utilization of Carbon-Based Energy Resources Jointly Built by Xinjiang Uyghur Autonomous Region and Ministry of Science and Technology, Xinjiang University, Urumqi 830046, Xinjiang, P. R. China. E-mail: zhongmei0504@126.com.*
[b.] *Ningbo Institute of Materials Technology and Engineering, Chinese Academy of Sciences, Ningbo 315201, Zhejiang, P. R. China. E-mail: wangshiwei@nimte.ac.cn*
[c.] *Xinjiang Key Laboratory of Coal Clean Conversion & Chemical Engineering Process, School of Chemical Engineering and Technology, Xinjiang University, Urumqi 830046, Xinjiang, P. R. China.*
[d.] *Yankuang Xinjiang Coal Chemical Co., Ltd., Urumqi 831408, Xinjiang, P. R. China.*
† Electronic Supplementary Information (ESI) available. See
DOI: 10.1039/x0xx00000x

Table S1. Molecular weights and polydispersity indexes of SAF-*t* and PSAF-*t* dispersants.

Samples	M_w (Da)	M_n (Da)	PDI
SAF-4	53123	14105	3.77
SAF-6	57240	14562	3.93
SAF-8	62796	15577	4.03
PSAF-4	11189	6153	1.82
PSAF-6	11787	6415	1.84
PSAF-8	6758	4413	1.53

Table S1 summarized molecular weights and PDI of the SAF-*t* and PSAF-*t* samples. Obviously, the molecular weights of SAF-*t* dispersants are higher than that of PSAF-*t* dispersants. The PDI of PSAF-*t* are lower than that of SAF-*t*, indicating that molecular weight distribution of which are narrower.

Table S2. Rheological parameter values of CWS fitted by Herschel–Bulkley model.

Dispersants	τ_y (Pa)	K (Pa·s^n)	n	R^2
SAF-4	-0.40	1.00	0.85	0.9992
SAF-6	0.64	0.81	0.90	0.9999
SAF-8	0.04	1.00	0.86	0.9998
PSAF-4	-1.07	0.92	0.83	0.9977
PSAF-6	-1.62	1.08	0.78	0.9978
PSAF-8	-0.86	0.88	0.85	0.9975

Table S2 summarized rheological parameter values of CWS prepared by PSAF-*t* and SAF-*t* dispersants. The rheological index, n, was less than 1, indicating again that the non-Newtonian pseudoplastic behaviors of CWS. Moreover, the τ_y of CWS with PSAF-6 was the lowest compared with others. It means that it has stronger dispersing ability.

Table S3. The Langmuir fitting parameters of adsorption curves.

Dispersants	Γ_∞（mg·g^{-1}）	k	R^2
SAF-4	1.47	3.96×10^{-3}	0.981
PSAF-6	3.50	3.24×10^{-3}	0.981

As presented in Table S3, the correlation coefficients (R^2) of Langmuir equation for dispersants were 0.981. It shows that Langmuir adsorption model can describe the adsorption of dispersants on the surface of coal particles properly and shows the characteristics of monolayer adsorption. The saturated adsorption capacity of SAF-4 on coal surface is lower than that of PSAF-6.

Table S4. Si_{2p} XPS of the original coal, coal@SAF-4 and coal@PSAF-6.

Samples	Binding energy(eV)	Photoelectron intensity(cps)	Adsorption layer thickness (nm)
Original Coal	100.7	575.4	/
Coal@SAF-4	100.4	463.9	0.9
Coal@PSAF-6	100.6	243.9	3.5

Table S4 presented Si_{2p} photoelectron intensity and calculated adsorption layer thickness of coal, coal@SAF-4 and coal@PSAF-6 samples. The larger adsorption layer thickness for PSAF-6 than SAF-4, which is consistent with the results of adsorption capacity.

Table S5. Distribution ratio of adsorption water, interstitial water and free water of CWS.

Type of CWS	Proportion of f_1 (%)	Proportion of f_2(%)	Proportion of f_3(%)
Blank	15.21	82.93	1.86
SAF-4	18.01	81.90	0.10
PSAF-6	15.31	84.65	0.04

The distribution ratio of water in different state were summarized in Table S5. The free water content of CWS prepared with dispersants are obviously lower than that of CWS prepared without dispersant. This phenomenon indicates that the free water in composite particles to be converted into adsorbed water or interstitial water. Compared with SAF-4, the coal water slurry prepared by PSAF-6 has lower adsorbed water content and higher interstitial water content.

Table S6. Molecular weights and polydispersity indexes of SAF-4, PSAF-6, o-PSAF-6, d-PSAF-6, m-PSAF-6, c-PSAF-6.

Samples	M_w (Da)	M_n (Da)	PDI
SAF-4	53123	14105	3.77
PSAF-6	11787	6415	1.84
o-PSAF-6	12154	5746	2.12
d-PSAF-6	13955	7157	1.95
m-PSAF-6	13440	6564	2.05
c-PSAF-6	16095	7525	2.14

Table S6 summarized molecular weights and polydispersity indexes of SAF-4, PSAF-6, o-PSAF-6, d-PSAF-6, m-PSAF-6, c-PSAF-6 samples. The molecular weight of *x*-PSAF-6 dispersant is comparable to that of PSAF-6, but lower than that of SAF-4.

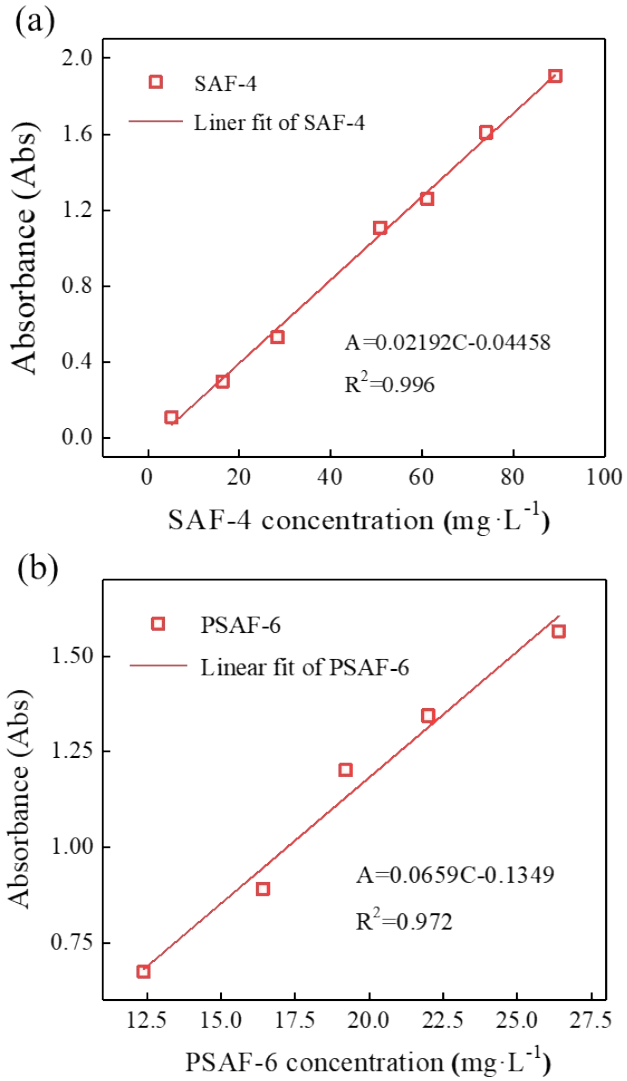

Figure S1. Calibration curve of SAF-4 (a) and PSAF-6 (b) dispersants.
Figure S1 shows that strong correlation between the concentration of dispersants and absorbance.

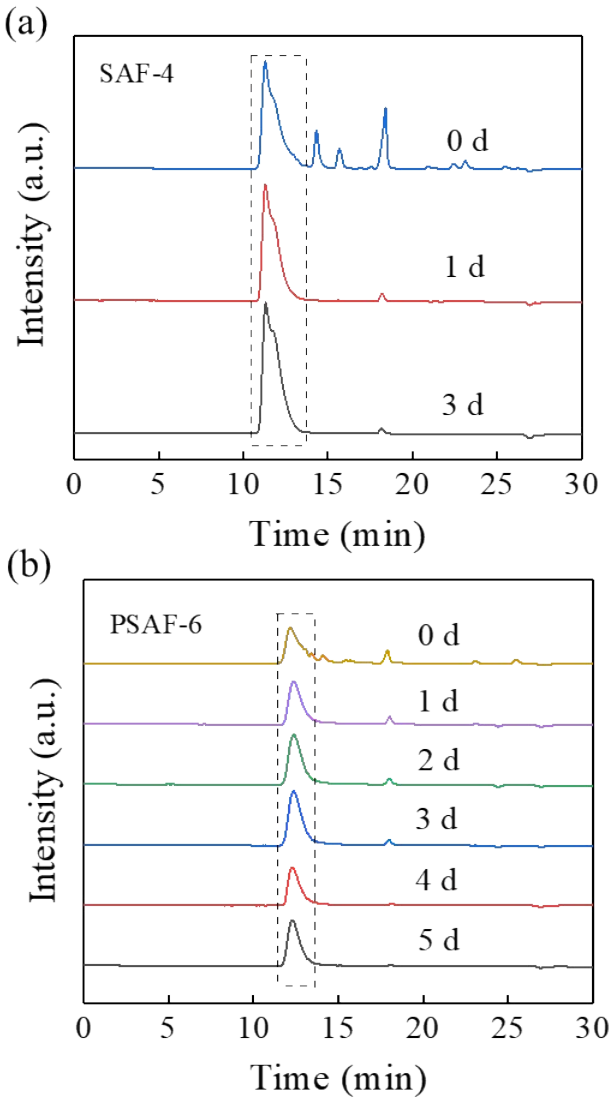

Figure S2. Gel permeation chromatography (GPC) analysis for dialysis purification of SAF-4 (a) and PSAF-6 (b).
Figure S2 presented molecular weight distribution of PSAF-6 and SAF-4 dispersants. Obviously, unreacted monomers and prepolymers in PSAF-6 and SAF-4 dispersants were basically removed after 5 and 3 days of dialysis, respectively.

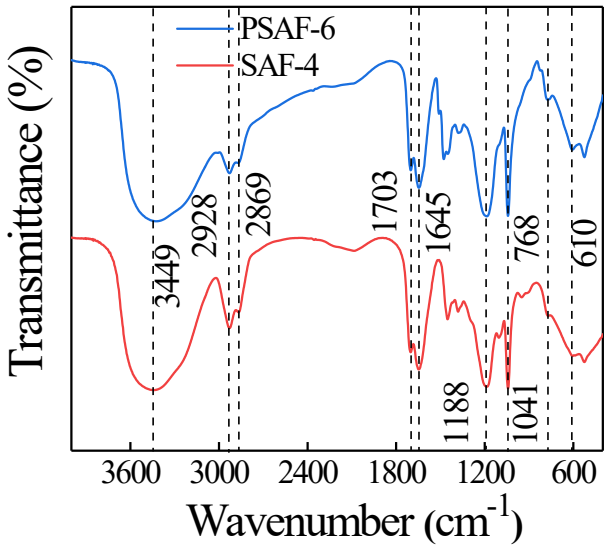

Figure S3. FT-IR spectra of PSAF-6 and SAF-4.
As shown in Figure S3, PSAF-6 and SAF-4 dispersants contained O-H (3449 cm^{-1}), C-H (2928 and 2869 cm^{-1}), C=O (1703 cm^{-1}), C=C (1645 cm^{-1}), S=O (1188 cm^{-1}) and S-O (1041 cm^{-1}) and C-S (768 and 610 cm^{-1}). Unlike SAF-4, the PSAF-6 dispersant contains vibration absorption peaks of benzene ring skeleton (1512 and 1476 cm^{-1}), which indicates that phenol structural units have been successfully introduced into the aliphatic molecular chain.

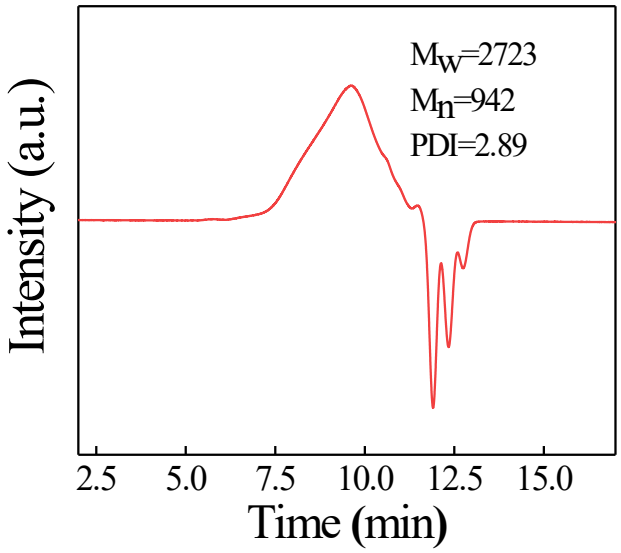

Figure S4. Gel permeation chromatography (GPC) analysis for reaction product of formaldehyde and acetone.
As shown in Figure S4, reaction product of formaldehyde and acetone gives M_W of 2723 Da, which indicate that formaldehyde and acetone could be polymerized under catalysis of OH^-.

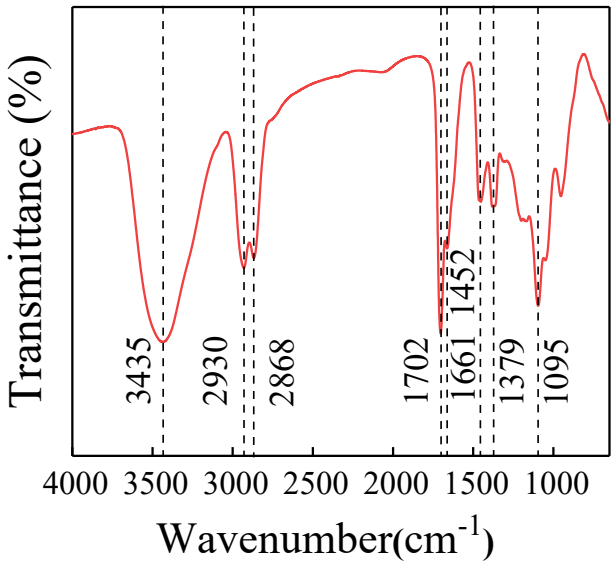

Figure S5. FT-IR spectra of product of formaldehyde and acetone.
Figure S5 represents infrared characteristic peaks of polymerization product. The peaks at 2930 cm^{-1} and 2868 cm^{-1} result from stretching vibration of C-H, and bending vibrations of which appears at 1452 cm^{-1} and 1379 cm^{-1}. The characteristic peak of O-H appears at 3435 cm^{-1}, while peaks at 1702 cm^{-1} and 1095 cm^{-1} can be assigned to stretching vibration of C=O and C-O, respectively. Significantly, the characteristic peak of C=C appear at 1661 cm^{-1} indicating that this polymer contains C=C groups.

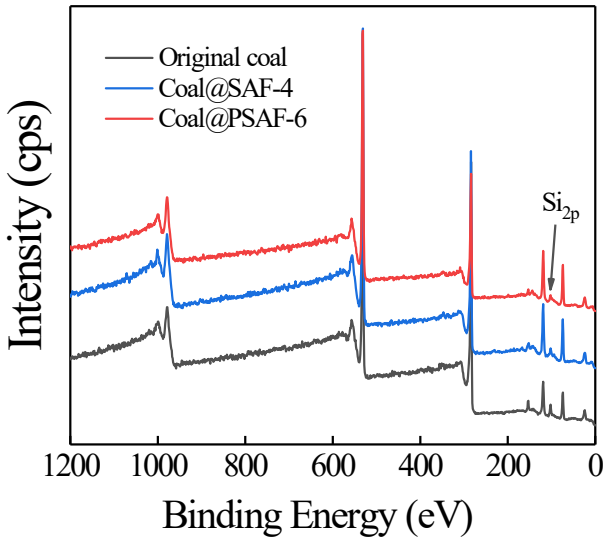

Figure S6. XPS scanning spectra of original coal, coal@SAF-4 and coal@PSAF-6.
XPS scanning spectra of original coal, coal@SAF-4 and coal@PSAF-6. Elemental scanning spectra of Yulin coal before and after absorbing dispersants SAF-4 and PSAF-6 were depicted by XPS in Figure S6. Compared with original coal sample, the intensity of Si peaks on the surface of coal after absorbing SAF-4 and PSAF-6 decreased. Though there were no Si in SAF-4 and PSAF-6, Si element was still detected on the coal surface due to the thin absorbed layer.

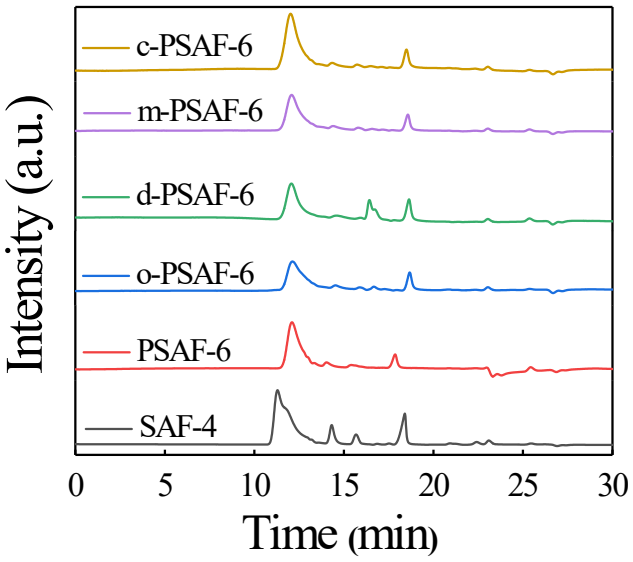

Figure S7. Gel permeation chromatography (GPC) analysis for SAF-4, PSAF-6 and *x*-PSAF-6 dispersants.
As shown in Figure S7, the SAF-4, PSAF-6 and *x*-PSAF-6 contain some unreacted monomers or small molecular polymers.

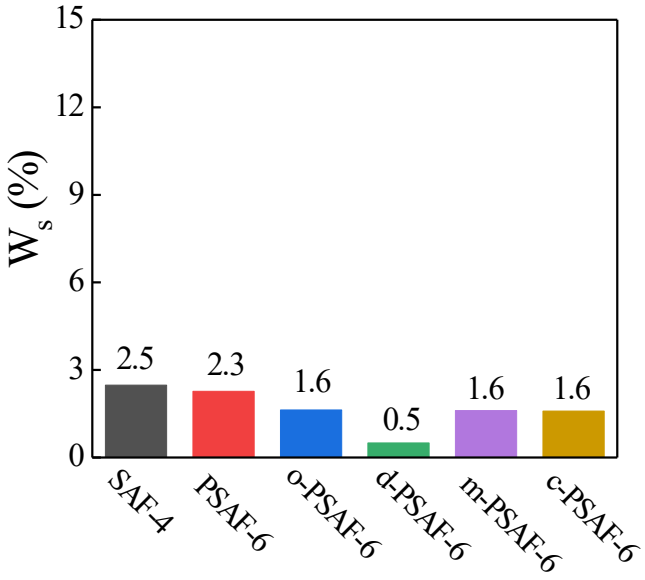

Figure S8. The water separating ratio of CWS prepared using SAF-4, PSAF-6, *x*-PSAF-6 dispersants.
The water separating ratio of CWS prepared from SAF-4, PSAF-6, *x*-PSAF-6 are shown in Figure S8. In general, the CWS prepared from PSAF-6 and *x*-PSAF-6 show lower water separating ratio than that from SAF-4. It is worth noting that the water separating ratio of m-PSAF-6 and c-PSAF-6 are the same, indicating that m-PSAF-6 is reasonable as a model compound of c-PSAF-6.